11th US NATIONAL CONGRESS
ON COMPUTATIONAL MECHANICS

Minneapolis, July 24th-28th, 2011

On Dynamic Stability Evaluation of Functionally Graded Risers

C. A. Almeida*, G. H. Paulino, I. F. M. Menezes* and J. C. Romero***

***Pontifical Catholic University of Rio de Janeiro (PUC-Rio),**

calmeida@mec.puc-rio.br, ivan@tecgraf.puc-rio.br, jromeroal@hotmail.com,

****University of Illinois at Urbana-Champaign, Newmark Laboratory(UIUC)**

paulino@uiuc.edu

Presentation Outline

- Introduction
- F E Model Formulation
- Model for a FGM Riser
- Testing Examples
- Conclusions

Introduction

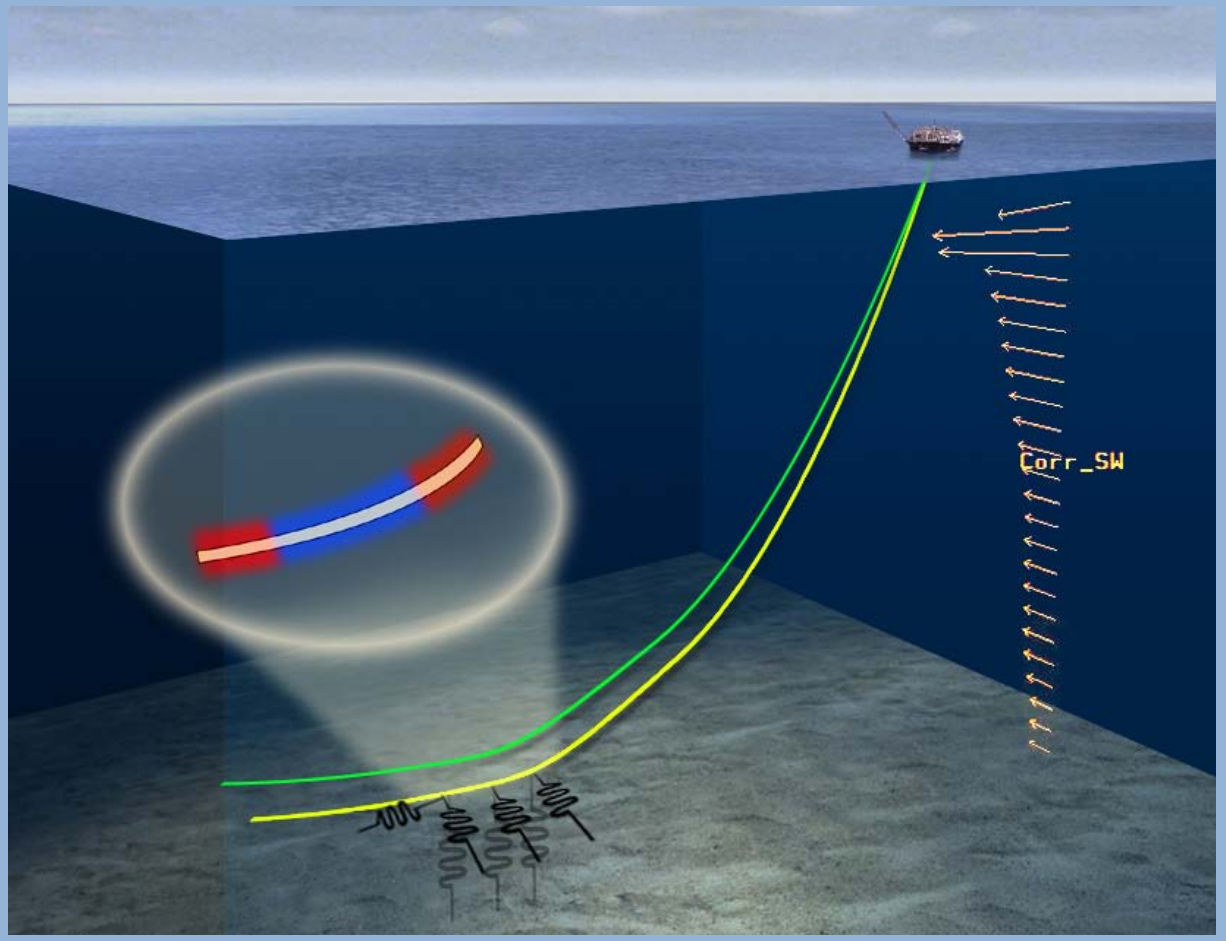

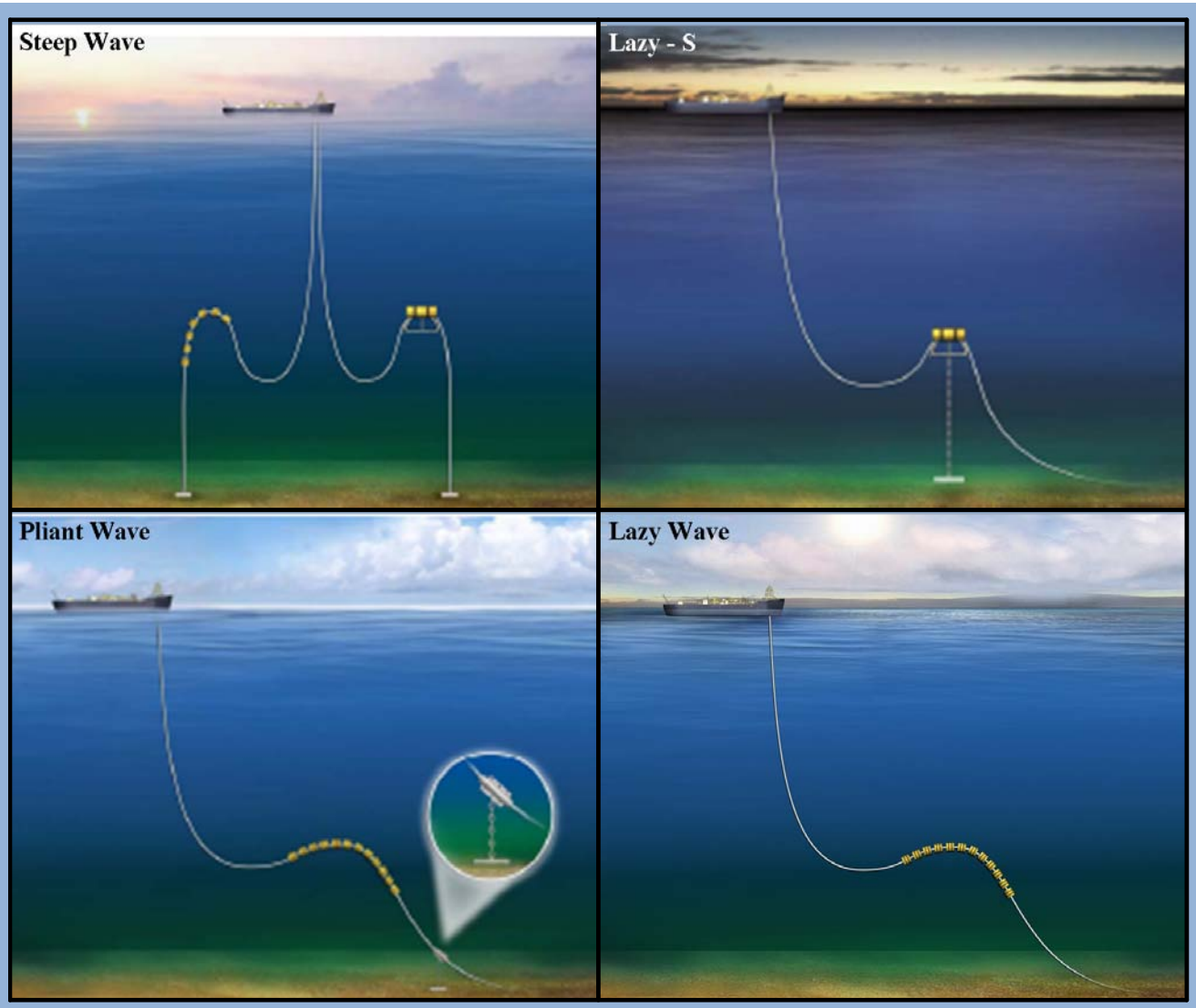
Steep Wave
Lazy - S
Pliant Wave
Lazy Wave

Flexible Risers Should Provide

- Easy and Effective Fluid and Gas Transport
- Signal Transmission Capabilities
- Power Supply to Sub-sea Components
- Compliance and High Deformability in Bending
- Strong and Stiff Response to: Internal and External Pressures, Tension and Torsion

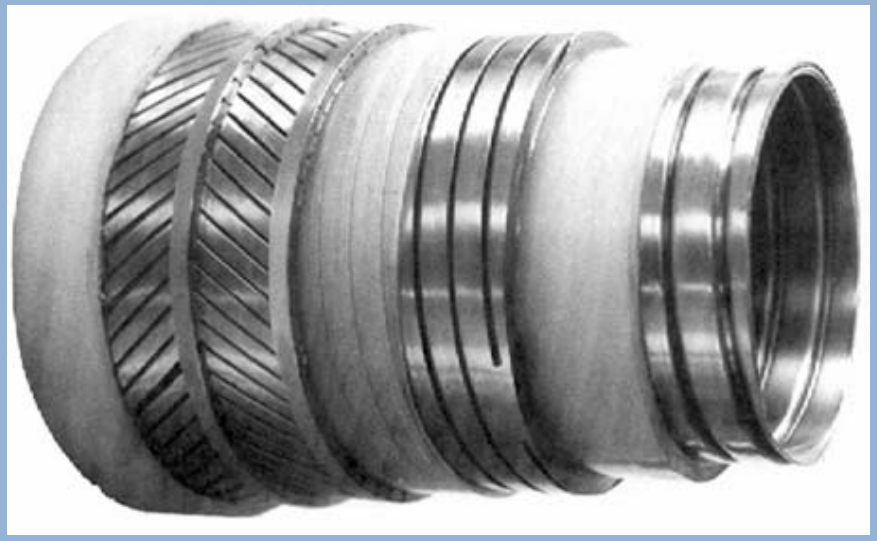

Flexible Riser – Concentric Polymeric & Interlocking Metallic Layers

F E Model Formulation

Co-rotational frame for a deformed beam element

Configurations:

- Initial configuration $\mathbf{C}_0$.
- Co-rotated configuration $\mathbf{C}_C$.
- Deformed configuration $\mathbf{C}_D$.

Coordinate systems:

- Global frame x_G, y_G, z_G
- Element base frame x_0, y_0, z_0
- Co-rotated frame x_C, y_C, z_C

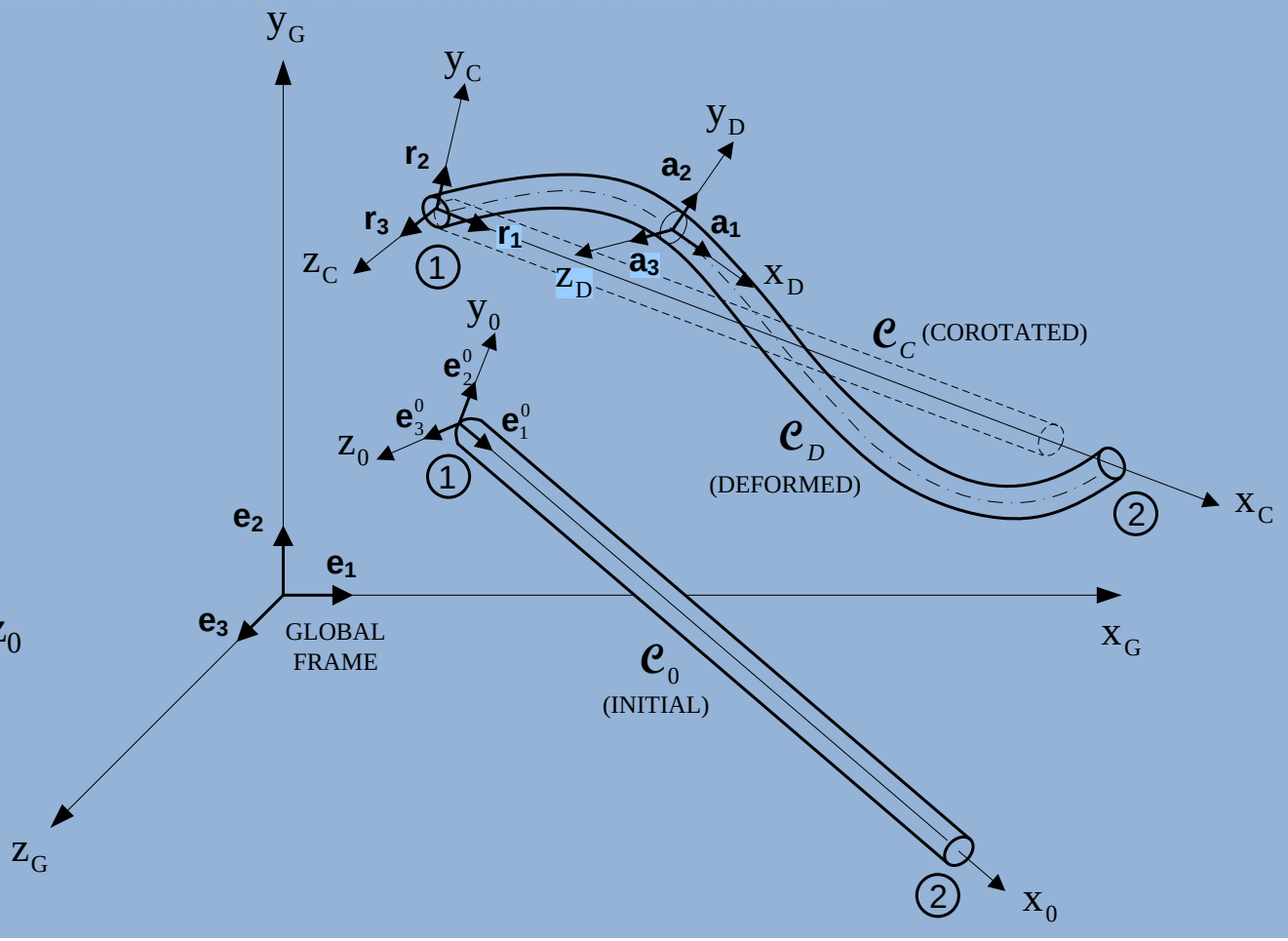

Local Beam Kinematics

Displacement increment vector

$$\mathbf{u}_P = \mathbf{X}_P - \mathbf{X}_P^0$$

where

$$\mathbf{X}_P^0 = \mathbf{X}_G^0 + x_2\mathbf{r}_2 + x_3\mathbf{r}_3$$

$$\mathbf{X}_P = \mathbf{X}_G + x_2\mathbf{a}_2 + x_3\mathbf{a}_3$$

then

$$\mathbf{u}_P = \mathbf{X}_P - \mathbf{X}_P^0 = \mathbf{X}_G - \mathbf{X}_G^0 + x_2\left(\mathbf{a}_2 - \mathbf{r}_2\right) + x_3\left(\mathbf{a}_3 - \mathbf{r}_3\right)$$

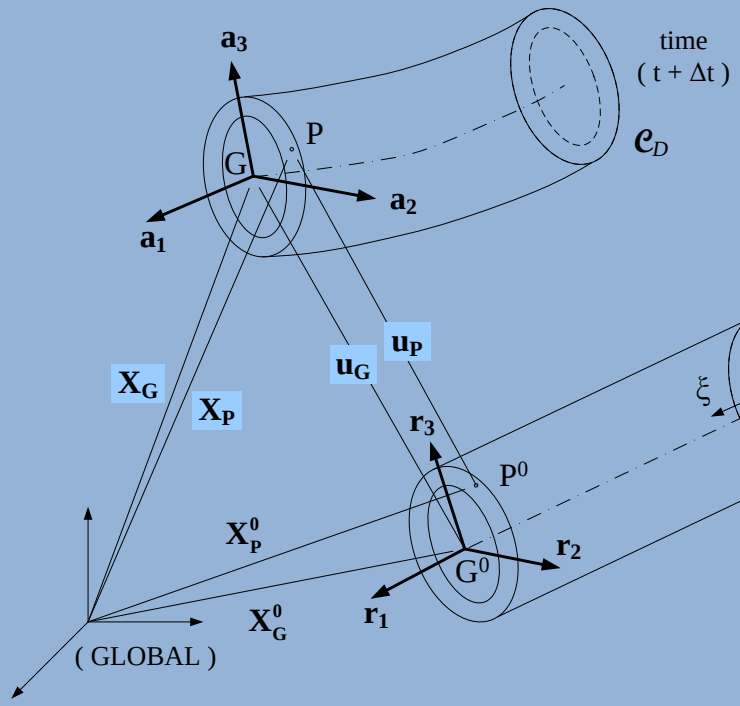

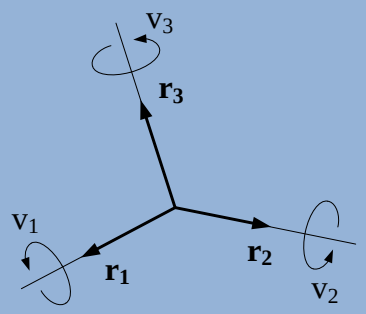

Rotation matrix

$\mathbf{a}_i = \mathbf{R}_i$, (i = 1,2,3)

$$\boldsymbol{\Psi} = v_1\mathbf{r}_1 + v_2\mathbf{r}_2 + v_3\mathbf{r}_3 = \begin{bmatrix} v_1 \\ v_2 \\ v_3 \end{bmatrix} = \mathbf{e}\,\psi$$

Rotational vector

$$\psi = \sqrt{v_1^2 + v_2^2 + v_3^2}$$

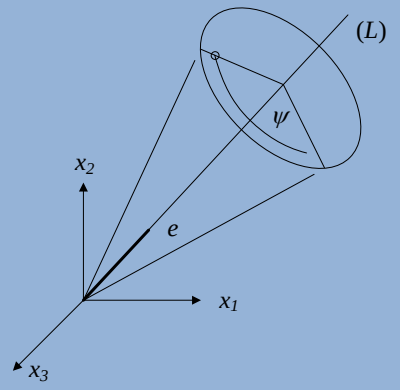

In terms of $\boldsymbol{\Psi}$, the orthogonal matrix $\mathbf{R}$ admits the following representation:

$$\mathbf{R} = \mathbf{I} + \frac{sen\,\psi}{\psi}\mathbf{S}(\boldsymbol{\Psi}) + \frac{1}{2}\left[\frac{sen(\psi/2)}{\psi/2}\right]^2 \mathbf{S}(\boldsymbol{\Psi})\,\mathbf{S}(\boldsymbol{\Psi}) \quad \text{,where} \quad \mathbf{S}(\boldsymbol{\Psi}) = \begin{bmatrix} 0 & -v_3 & v_2 \\ v_3 & 0 & -v_1 \\ -v_3 & v_1 & 0 \end{bmatrix}$$

If the trigonometric functions in the above equation are expanded in Taylor series and using a second-order approximation of $\mathbf{R}$

$$\mathbf{R} = \mathbf{I} + \mathbf{S}(\boldsymbol{\Psi}) + \frac{1}{2}\mathbf{S}(\boldsymbol{\Psi})\,\mathbf{S}(\boldsymbol{\Psi}) \quad \mathbf{R} \;, \quad = \begin{bmatrix} 1 - \frac{v_2^2 + v_3^2}{2} & -v_3 + \frac{v_1 v_2}{2} & v_2 + \frac{v_1 v_3}{2} \\ v_3 + \frac{v_1 v_2}{2} & 1 - \frac{v_1^2 + v_3^2}{2} & -v_1 + \frac{v_2 v_3}{2} \\ -v_2 + \frac{v_1 v_3}{2} & v_1 + \frac{v_2 v_3}{2} & 1 - \frac{v_1^2 + v_2^2}{2} \end{bmatrix}$$

A second-order approximation of the displacement increment vector $\mathbf{u}_P$

$$u_{P_1} = u_1 - x_2 v_3 + x_3 v_2 + \frac{1}{2} x_2 v_1 v_2 + \frac{1}{2} x_3 v_1 v_3$$

$$u_{P_2} = u_2 \qquad - x_3 v_1 - \frac{1}{2} x_2 \left(v_1^2 + v_3^2 \right) + \frac{1}{2} x_3 v_2 v_3$$

$$u_{P_3} = \underbrace{u_3 + x_2 v_1}_{\text{linear}} + \underbrace{\frac{1}{2} x_2 v_2 v_3 - \frac{1}{2} x_3 \left(v_1^2 + v_2^2 \right)}_{\text{não-linear}}$$

With respect to the local system $\mathbf{r}_i$, the Green–Lagrange strain components which contribute to the strain energy of the beam are given by

$$\varepsilon_{11} = u_{P_{1,1}} \qquad + \frac{1}{2} \left(u_{P_{1,1}} \right)^2 + \frac{1}{2} \left(u_{P_{2,1}} \right)^2 + \frac{1}{2} \left(u_{P_{3,1}} \right)^2$$

$$\gamma_{12} = u_{P_{1,2}} + u_{P_{2,1}} + u_{P_{1,1}} u_{P_{1,2}} + u_{P_{2,1}} u_{P_{2,2}} + u_{P_{3,1}} u_{P_{3,2}}$$

$$\gamma_{13} = \underbrace{u_{P_{1,3}} + u_{P_{3,1}}}_{\text{linear}} + \underbrace{u_{P_{1,1}} u_{P_{1,3}} + u_{P_{2,1}} u_{P_{2,3}} + u_{P_{3,1}} u_{P_{3,3}}}_{\text{não-linear}}$$

$$\varepsilon_{11} = u_{1,1} - x_2 v_{3,1} + x_3 v_{2,1} + \frac{1}{2} \left(u_{2,1}^2 + u_{3,1}^2 \right) + x_2 \left[\frac{1}{2} \left(v_{1,1} v_2 + v_1 v_{2,1} \right) + u_{3,1} v_{1,1} \right]$$
$$+ x_3 \left[\frac{1}{2} \left(v_{1,1} v_3 + v_1 v_{3,1} \right) - u_{2,1} v_{1,1} \right] + \frac{1}{2} \left(x_2^2 + x_3^2 \right) v_{1,1}^2$$
$$+ \frac{1}{2} \left(x_2^2 v_{3,1}^2 + x_3^2 v_{2,1}^2 \right) - \left(x_2 x_3 \right) v_{3,1} v_{2,1}$$

$$\gamma_{12} = u_{2,1} - v_3 - x_3 v_{1,1} \qquad + \qquad \frac{1}{2} v_1 v_2 + u_{3,1} v_1 - \frac{1}{2} x_3 \left(v_{2,1} v_3 - v_2 v_{3,1} \right)$$

$$\gamma_{13} = \underbrace{u_{3,1} + v_2 + x_2 v_{1,1}}_{\text{linear } (e_{ij})} + \underbrace{\frac{1}{2} v_1 v_3 - u_{2,1} v_1 + \frac{1}{2} x_2 \left(v_{2,1} v_3 - v_2 v_{3,1} \right)}_{\text{não-linear } (\eta_{ij})}$$

Linearization of the Principle of Virtual Work

Principle of virtual displacements in the co-rotational updated Lagrange formulation

$$\int_{{}^tV} {}^{t+\Delta t}_{\ t}S_{ij}\ \delta\, {}^{t+\Delta t}_{\ t}\varepsilon_{ij}\ d\,{}^tV = {}^{t+\Delta t}\Re \qquad \text{,where} \qquad {}^{t+\Delta t}\Re = \int_{{}^0S} {}^{t+\Delta t}_{\ 0}f_i^S\ \delta u_i^S\ d\,{}^0S + \int_{{}^oV} {}^{t+\Delta t}_{\ 0}f_i^B\ \delta u_i\ d\,{}^0V$$

The following incremental decompositions are used

$${}^{t+\Delta t}_{\ t}S_{ij} = {}^t\tau_{ij} + {}_tS_{ij}$$

$${}^{t+\Delta t}_{\ t}\varepsilon_{ij} = {}^t_t\varepsilon_{ij} + {}_t\varepsilon_{ij}; \quad {}_t\varepsilon_{ij} = {}_te_{ij} + {}_t\eta_{ij}$$

then

$$\int_{{}^tV} \left({}^t\tau_{ij} + {}_tS_{ij}\right)\delta\left({}^t_t\varepsilon_{ij} + {}_te_{ij} + {}_t\eta_{ij}\right) d\,{}^tV = {}^{t+\Delta t}\Re$$

Using the approximations $\delta\,{}^t_t\varepsilon_{ij} = 0$, ${}_tS_{ij} = {}_tC_{ijrs}\ {}_te_{ij}$, we obtain as equation of motion

$$\int_{{}^tV} {}_tC_{ijrs}\ {}_te_{rs}\ \delta\,{}_te_{ij}\ d\,{}^tV + \int_{{}^tV} {}^t\tau_{ij}\ \delta\,{}_t\eta_{ij}\ d\,{}^tV = {}^{t+\Delta t}\Re - \int_{{}^tV} {}^t\tau_{ij}\ \delta\,{}_te_{ij}\ d\,{}^tV$$

Using d'Alembert principle and introducing the damping forces, we obtain the dynamic incremental equilibrium equation in the integral form

$$\int_{{}^oV} {}^0\rho\, {}^{t+\Delta t}\ddot{u}_i\ \delta u_i\ d\,{}^0V + \int_{{}^oV} c\, {}^{t+\Delta t}\dot{u}_i\ \delta u_i\ d\,{}^0V + \int_{{}^tV} {}_tC_{ijrs}\ {}_te_{rs}\ \delta\,{}_te_{ij}\ d\,{}^tV + \int_{{}^tV} {}^t\tau_{ij}\ \delta\,{}_t\eta_{ij}\ d\,{}^tV =$$

$$\int_{{}^0S} {}^{t+\Delta t}_{\ 0}f_i^S\ \delta u_i^S\ d\,{}^0S + \int_{{}^oV} {}^{t+\Delta t}_{\ 0}f_i^B\ \delta u_i\ d\,{}^0V - \int_{{}^tV} {}^t\tau_{ij}\ \delta\,{}_te_{ij}\ d\,{}^tV$$

Finite Element Discretization (Euler-Bernouilli Beam)

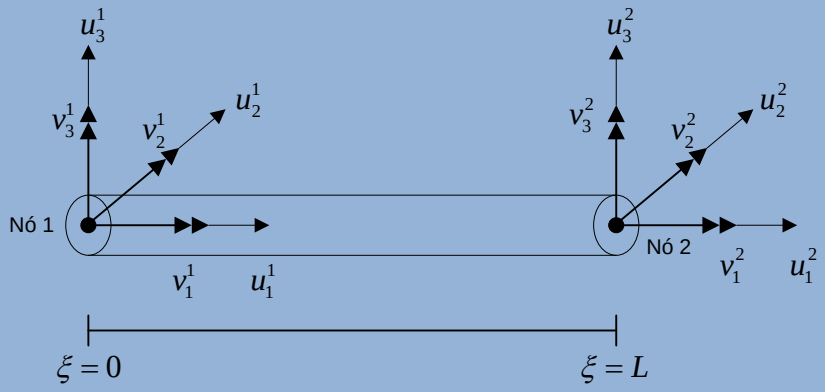

Using Hermite's interpolation functions

$$u_1(\xi) = \phi_1(\xi)u_1^1 + \phi_2(\xi)u_1^2$$
$$u_2(\xi) = \phi_3(\xi)u_2^1 + \phi_4(\xi)u_2^2 + \phi_5(\xi)v_3^1 - \phi_6(\xi)v_3^2$$
$$u_3(\xi) = \phi_3(\xi)u_3^1 + \phi_4(\xi)u_3^2 - \phi_5(\xi)v_2^1 + \phi_6(\xi)v_2^2$$
$$v_1(\xi) = \phi_1(\xi)v_1^1 + \phi_2(\xi)v_1^2$$
$$v_2(\xi) = -\phi_7(\xi)u_3^1 + \phi_7(\xi)u_3^2 + \phi_8(\xi)v_2^1 - \phi_9(\xi)v_2^2$$
$$v_3(\xi) = \phi_7(\xi)u_2^1 - \phi_7(\xi)u_2^2 + \phi_8(\xi)v_3^1 - \phi_9(\xi)v_3^2$$

where,

$$\phi_1(\xi) = 1-(\xi/\mathrm{L}), \quad \phi_2(\xi) = \xi/\mathrm{L}$$
$$\phi_3(\xi) = 1-3(\xi/\mathrm{L})^2 + 2(\xi/\mathrm{L})^3$$
$$\phi_4(\xi) = 3(\xi/\mathrm{L})^2 - 2(\xi/\mathrm{L})^3$$
$$\phi_5(\xi) = \left[(\xi/\mathrm{L}) - 2(\xi/\mathrm{L})^2 + (\xi/\mathrm{L})^3\right]\mathrm{L}$$
$$\phi_6(\xi) = \left[(\xi/\mathrm{L})^2 - (\xi/\mathrm{L})^3\right]\mathrm{L}$$
$$\phi_7(\xi) = \frac{6}{\mathrm{L}}\left[(\xi/\mathrm{L}) - (\xi/\mathrm{L})^2\right]$$
$$\phi_8(\xi) = 1-4(\xi/\mathrm{L}) + 3(\xi/\mathrm{L})^2$$
$$\phi_9(\xi) = 2(\xi/\mathrm{L}) - 3(\xi/\mathrm{L})^2 \qquad \text{for} \qquad (0 \le \xi/\mathrm{L} \le +1)$$

Nodal displacement increment vector (translations and rotations)

$$\hat{\mathbf{u}}^T = \left[u_1^1 \;\; u_2^1 \;\; u_3^1 \;\; v_1^1 \;\; v_2^1 \;\; v_3^1 \;\; | \;\; u_1^2 \;\; u_2^2 \;\; u_3^2 \;\; v_1^2 \;\; v_2^2 \;\; v_3^2\right]$$

Finite Element Matrices

$$\int_{{}^0V} {}^0\rho\, {}^{t+\Delta t}\ddot{u}_i\, \delta u_i\, d\,{}^0V \qquad \mathbf{M}\,{}^{t+\Delta t}\ddot{\mathbf{U}} = \left[\sum_m \int_{{}^0V^{(m)}} \rho^{(m)}\mathbf{H}^{(m)T}\ {}^{t+\Delta t}_{0}\mathbf{H}^{B(m)}\, d\,{}^0V^{(m)}\right]{}^{t+\Delta t}\ddot{\mathbf{U}}$$

$$+ \qquad +$$

$$\int_{{}^0V} c\,{}^{t+\Delta t}\dot{u}_i\, \delta u_i\, d\,{}^0V \qquad \mathbf{C}\,{}^{t+\Delta t}\dot{\mathbf{U}} = \left[\sum_m \int_{{}^0V^{(m)}} c^{(m)}\mathbf{H}^{(m)T}\ {}^{t+\Delta t}_{0}\mathbf{H}^{B(m)}\, d\,{}^0V^{(m)}\right]{}^{t+\Delta t}\dot{\mathbf{U}}$$

$$+ \qquad +$$

$$\int_{{}^tV} {}_tC_{ijrs}\ {}_te_{rs}\ \delta\,{}_te_{ij}\, d\,{}^tV \qquad {}^t_t\mathbf{K}_L\mathbf{U} = \left[\sum_m \int_{{}^tV^{(m)}} {}^t_t\mathbf{B}_L^{(m)T}\ {}_t\mathbf{C}^{(m)}\ {}^t_t\mathbf{B}_L^{(m)}\, d\,{}^tV^{(m)}\right]\mathbf{U}$$

$$+ \qquad +$$

$$\int_{{}^tV} {}^t\tau_{ij}\ \delta\,{}_t\eta_{ij}\, d\,{}^tV \qquad {}^t_t\mathbf{K}_{NL}\mathbf{U} = \left[\sum_m \int_{{}^tV^{(m)}} {}^t_t\mathbf{B}_{NL}^{(m)T}\ {}^t\boldsymbol{\tau}^{(m)}\ {}^t_t\mathbf{B}_{NL}^{(m)}\, d\,{}^tV^{(m)}\right]\mathbf{U}$$

$$= \qquad =$$

$${}^{t+\Delta t}\Re = \int_{{}^0S} {}^{t+\Delta t}_{0}f_i^S\ \delta u_i^S\ d\,{}^0S \qquad {}^{t+\Delta t}\mathbf{R} = \sum_m \int_{{}^0S^{(m)}} \mathbf{H}^{S(m)T}\ {}^{t+\Delta t}_{0}\mathbf{f}^{S(m)}\, d\,{}^0S^{(m)}$$

$$+ \int_{{}^0V} {}^{t+\Delta t}_{0}f_i^B\ \delta u_i\, d\,{}^0V \qquad + \sum_m \int_{{}^0V^{(m)}} \mathbf{H}^{(m)T}\ {}^{t+\Delta t}_{0}\mathbf{f}^{B(m)}\, d\,{}^0V^{(m)}$$

$$- \qquad -$$

$$\int_{{}^tV} {}^t\tau_{ij}\ \delta\,{}_te_{ij}\, d\,{}^tV \qquad {}^t_t\mathbf{F} = \sum_m \int_{{}^tV^{(m)}} {}^t_t\mathbf{B}_L^{(m)T}\ {}^t\hat{\boldsymbol{\tau}}^{(m)}\ d\,{}^tV^{(m)}$$

Dynamic incremental equilibrium equation in the matrix form

$$\mathbf{M}\,{}^{t+\Delta t}\ddot{\mathbf{U}} + \mathbf{C}\,{}^{t+\Delta t}\dot{\mathbf{U}} + \left({}^t_t\mathbf{K}_L + {}^t_t\mathbf{K}_{NL}\right)\mathbf{U} = {}^{t+\Delta t}\mathbf{R} - {}^t_t\mathbf{F}$$

Model for a F G M Riser

$$ {}_t\mathbf{C}^{(m)} = \begin{bmatrix} E_0 r^{\beta} & 0 & 0 \\ 0 & \dfrac{E_0 r^{\beta}}{2(1+\nu)} & 0 \\ 0 & 0 & \dfrac{E_0 r^{\beta}}{2(1+\nu)} \end{bmatrix} $$

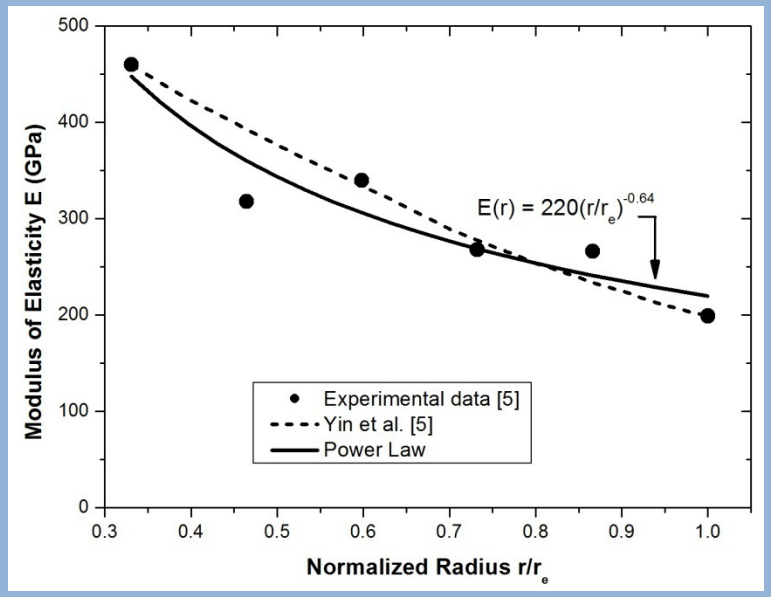

Power Law Approximation for FGM (TiC – Ni_3Al) Along Riser Thickness

Estimate of the power law

$$E = E_0 r^{\beta}$$

$$\ln E = \beta \ln r + \ln E_0$$

$$\left.\begin{aligned} y &= \ln E \\ m &= \beta \\ x &= \ln r \\ n &= \ln E_0 \end{aligned}\right\} \; y = mx + n$$

Least squares

$$m = \frac{NS_{xy} - S_x S_y}{NS_{xx} - S_x S_x}$$

$$n = \frac{S_{xx} S_y - S_x S_{xy}}{NS_{xx} - S_x S_x}$$

where

$$S_x = \sum_{i=1}^{N} x_i \qquad S_{xx} = \sum_{i=1}^{N} x_i^2$$

$$S_y = \sum_{i=1}^{N} y_i \qquad S_{xy} = \sum_{i=1}^{N} x_i y_i$$

then $\beta = m, \quad E_0 = e^n$

Testing Examples

- **Natural Frequency Evaluations of Composite Cross-Section Beams**

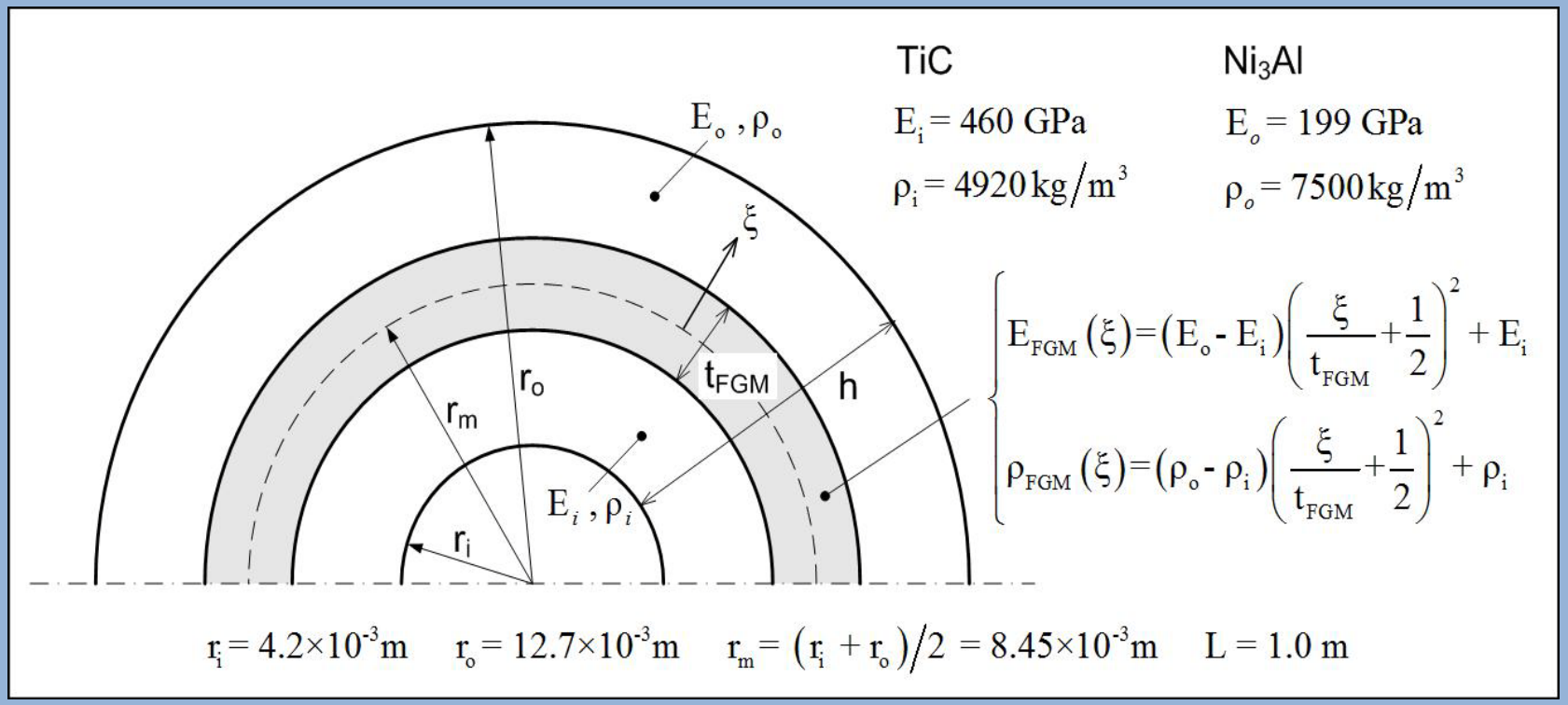

Composite Cross-Section Details as Considered in the Numerical Analysis

Testing Examples

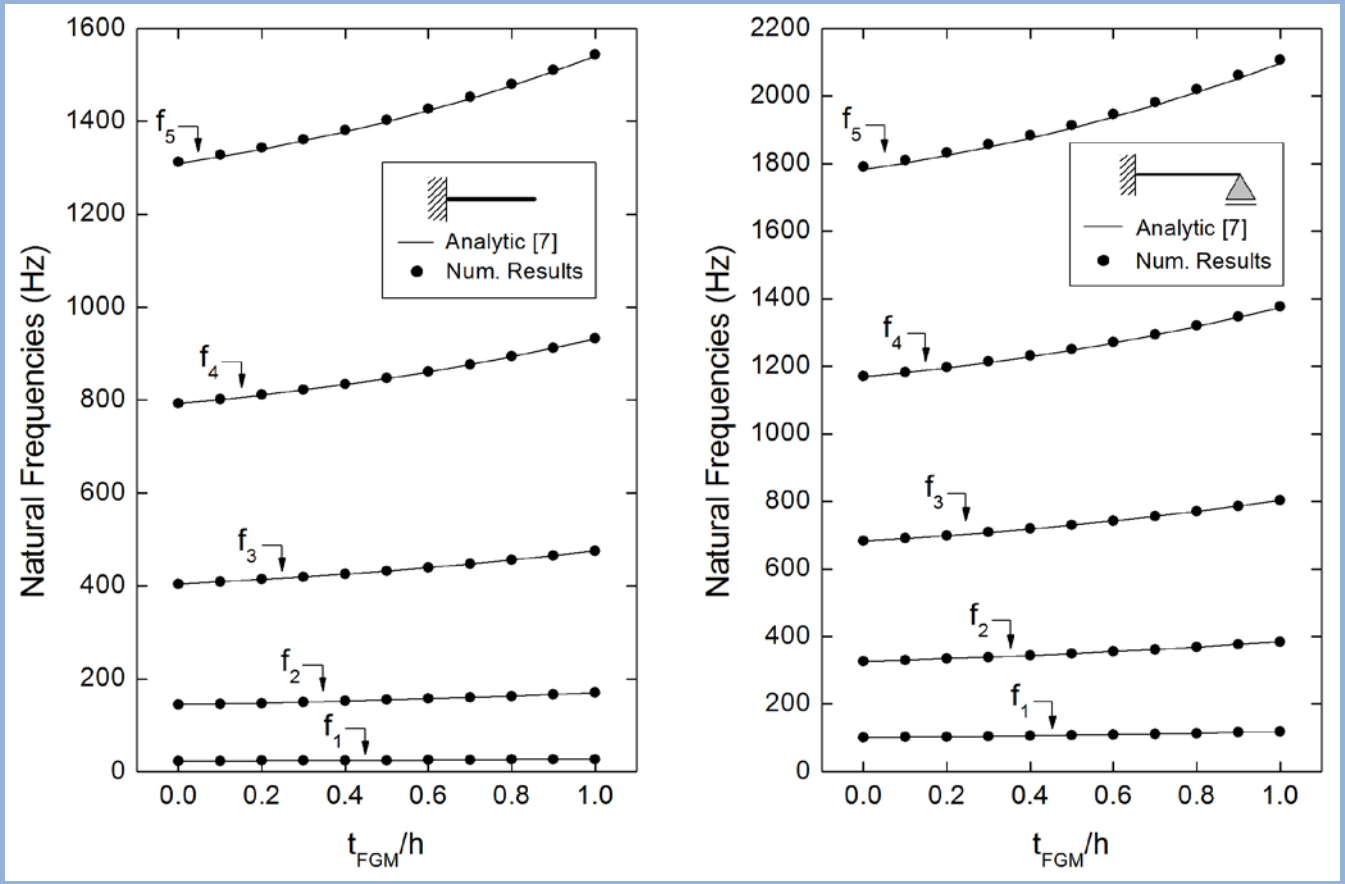

First Five Flexure Natural Frequencies Obtained For Composite Beams

Testing Examples

- **Cantilever Beam Under Buckling**

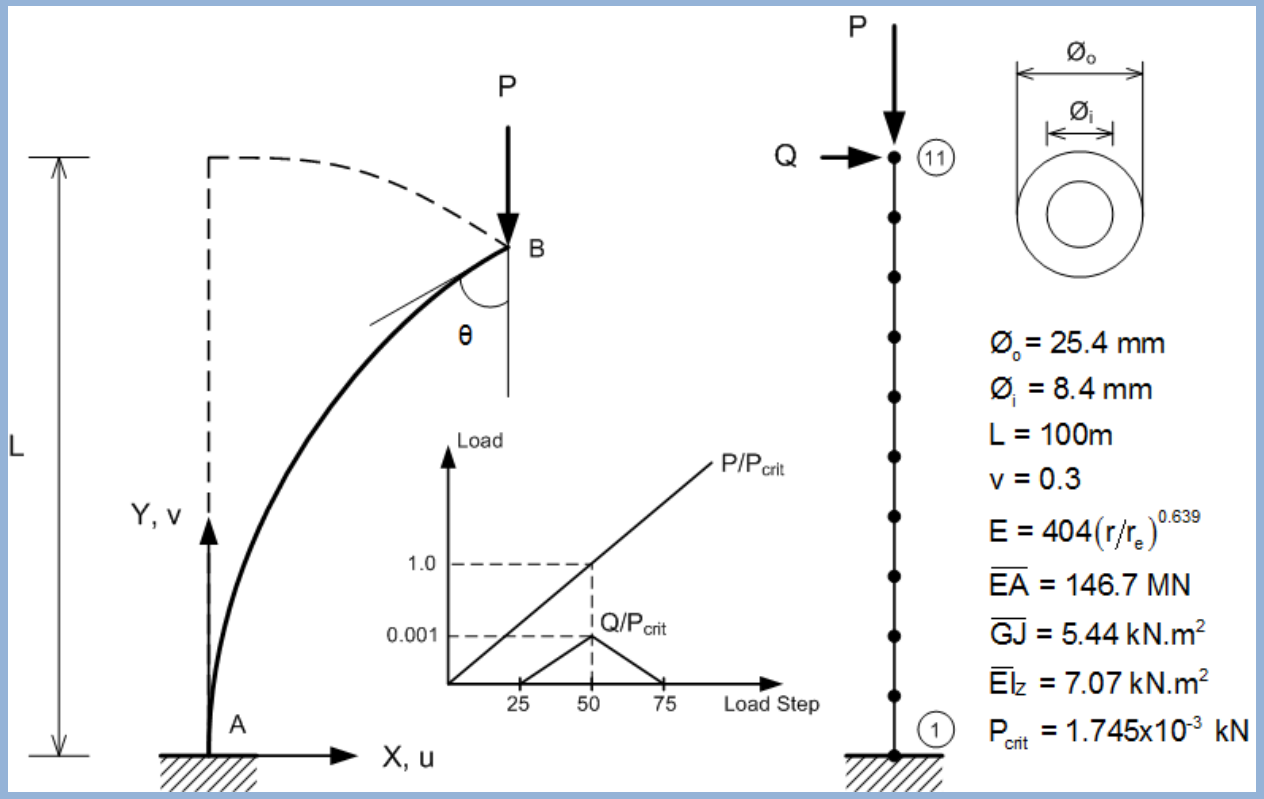

Beam Geometric, Physical and Loading Characteristics

Testing Examples

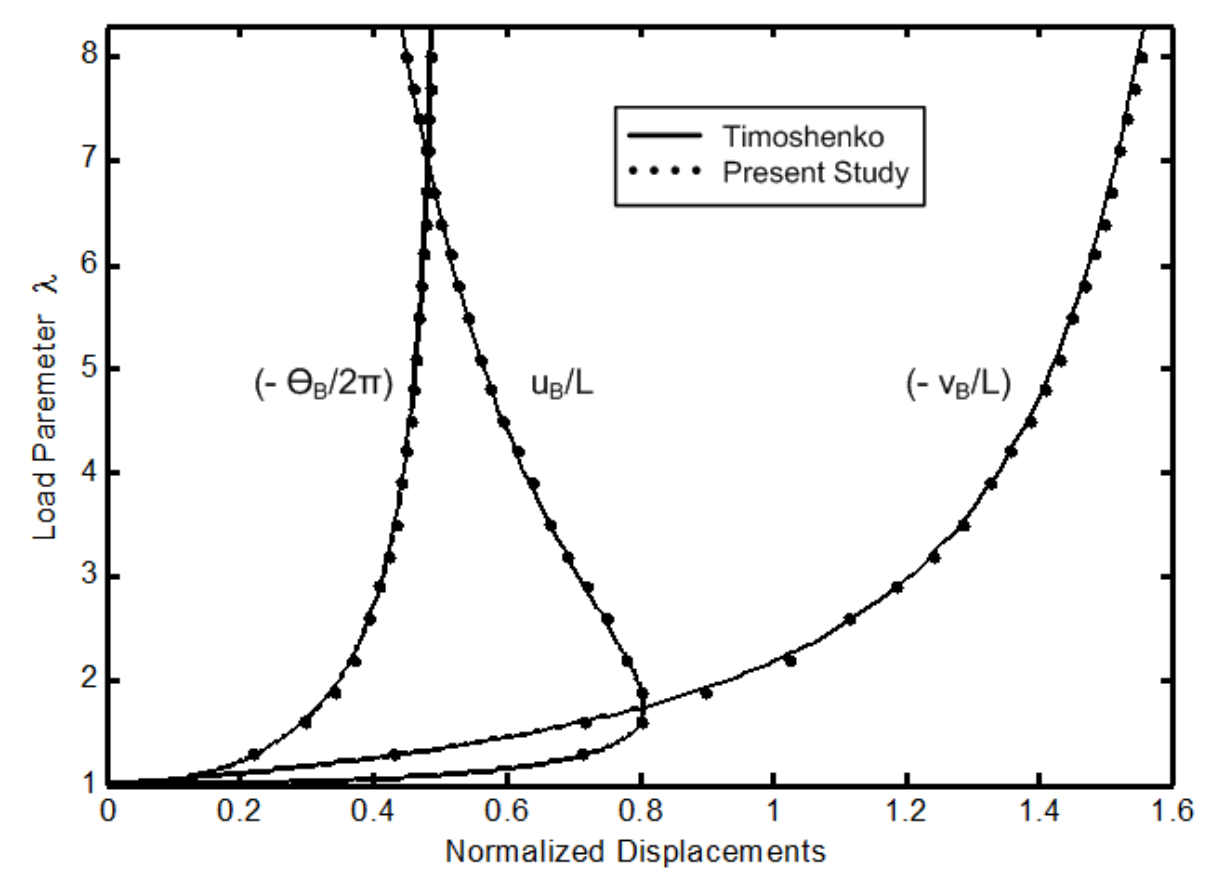

Normalized Numerical Displacements as Compared to Analytical Solutions

Testing Examples

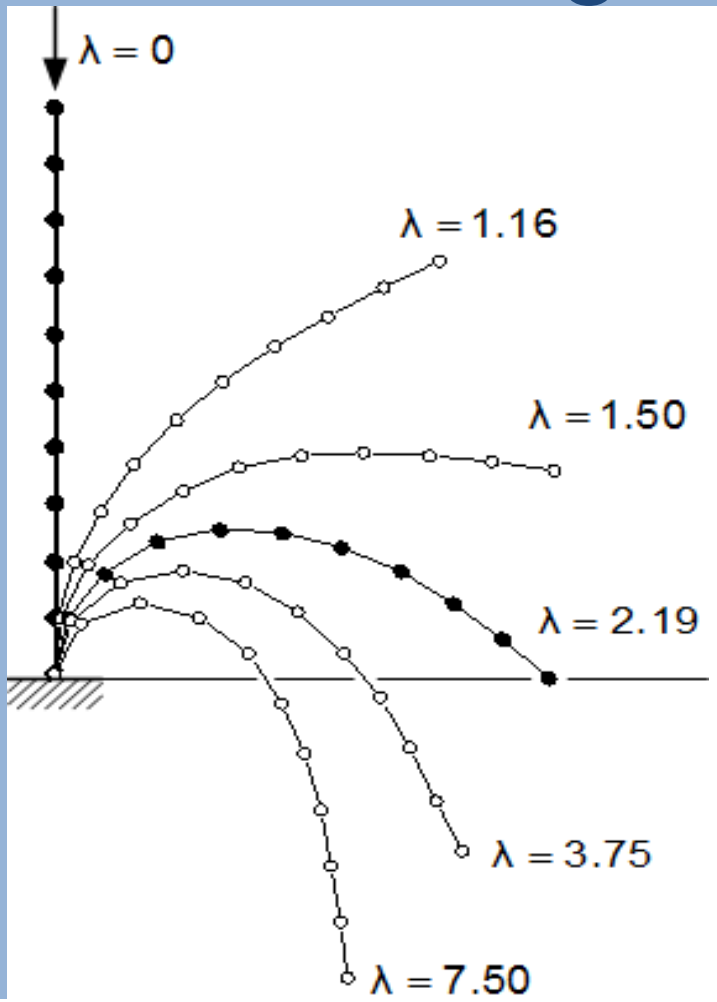

Beam Configurations For Various Tip Loadings

Testing Examples

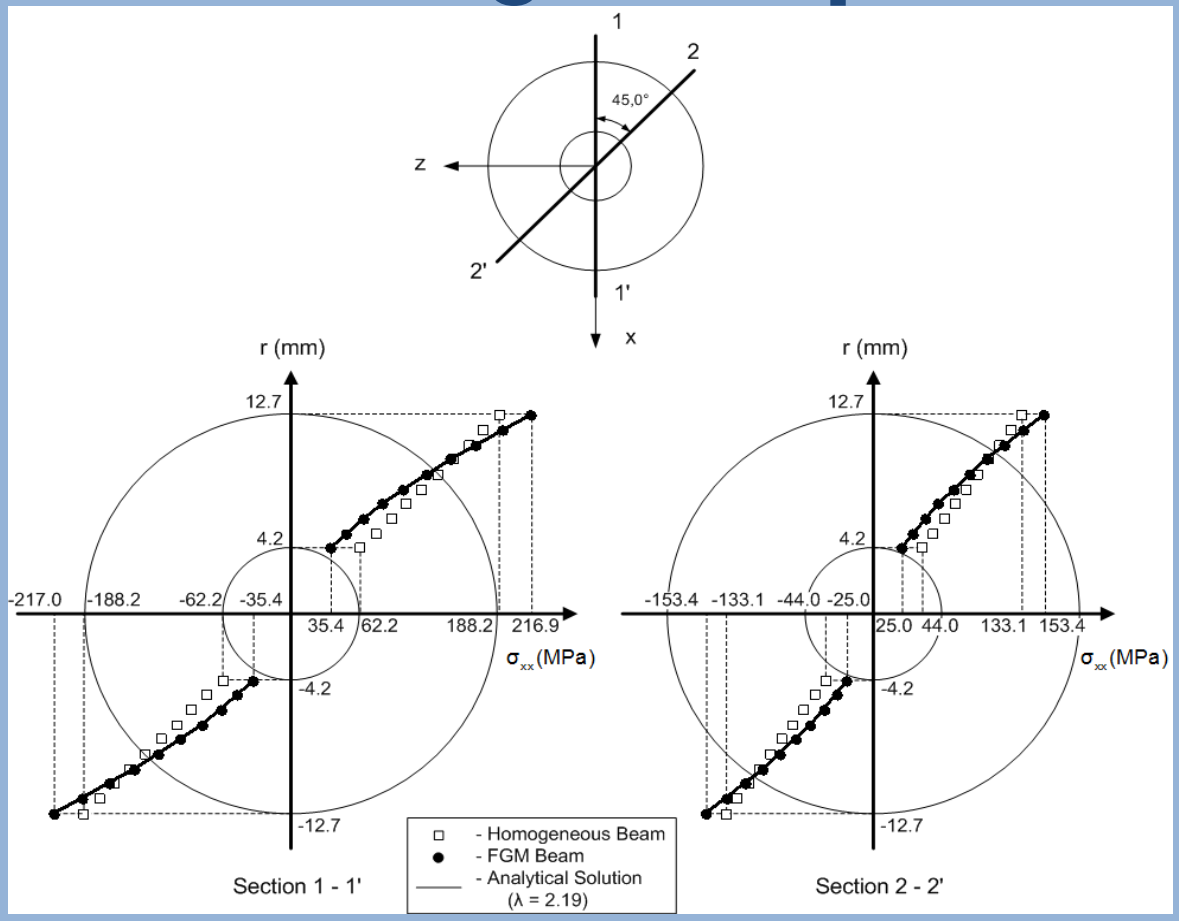

Normal Stresses at Beam Clamped End ($\lambda = 2.19$, $E(r) = 404(r/ro)^{0.64}$ GPa)

Testing Examples

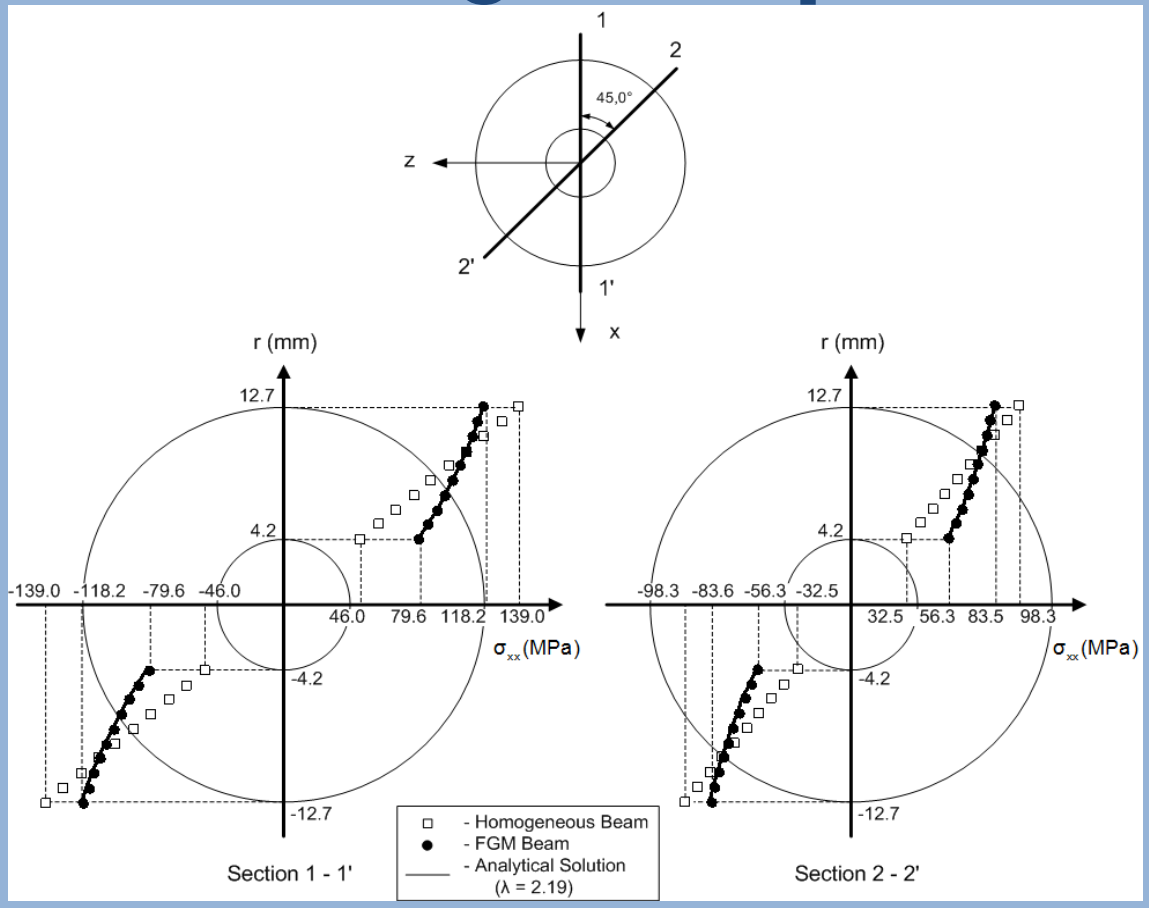

Normal Stresses at Beam Clamped End ($\lambda = 2.19$, $E(r) = 220(r/ro)^{-0.64}$ GPa)

Testing Examples

- **Cantilever Arch Beam Under Out-of-Plane Loading**

A - Static Analysis

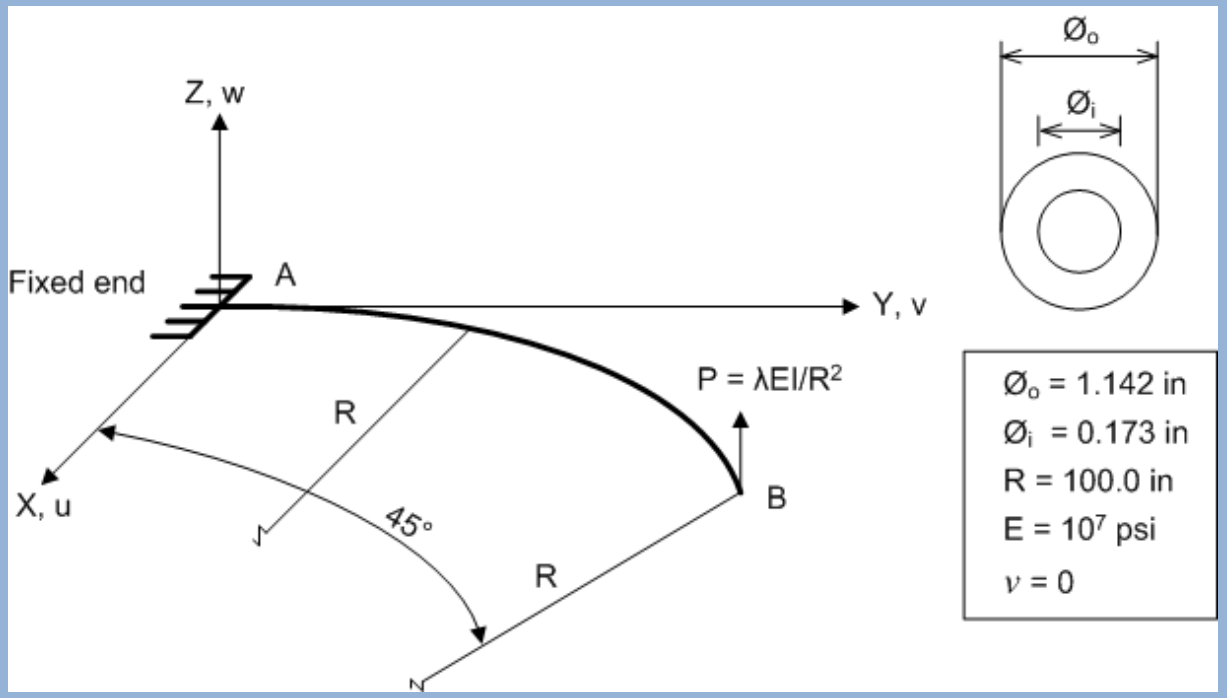

Beam Geometric, Material (Homogeneous) and Loading Characteristics

Testing Examples

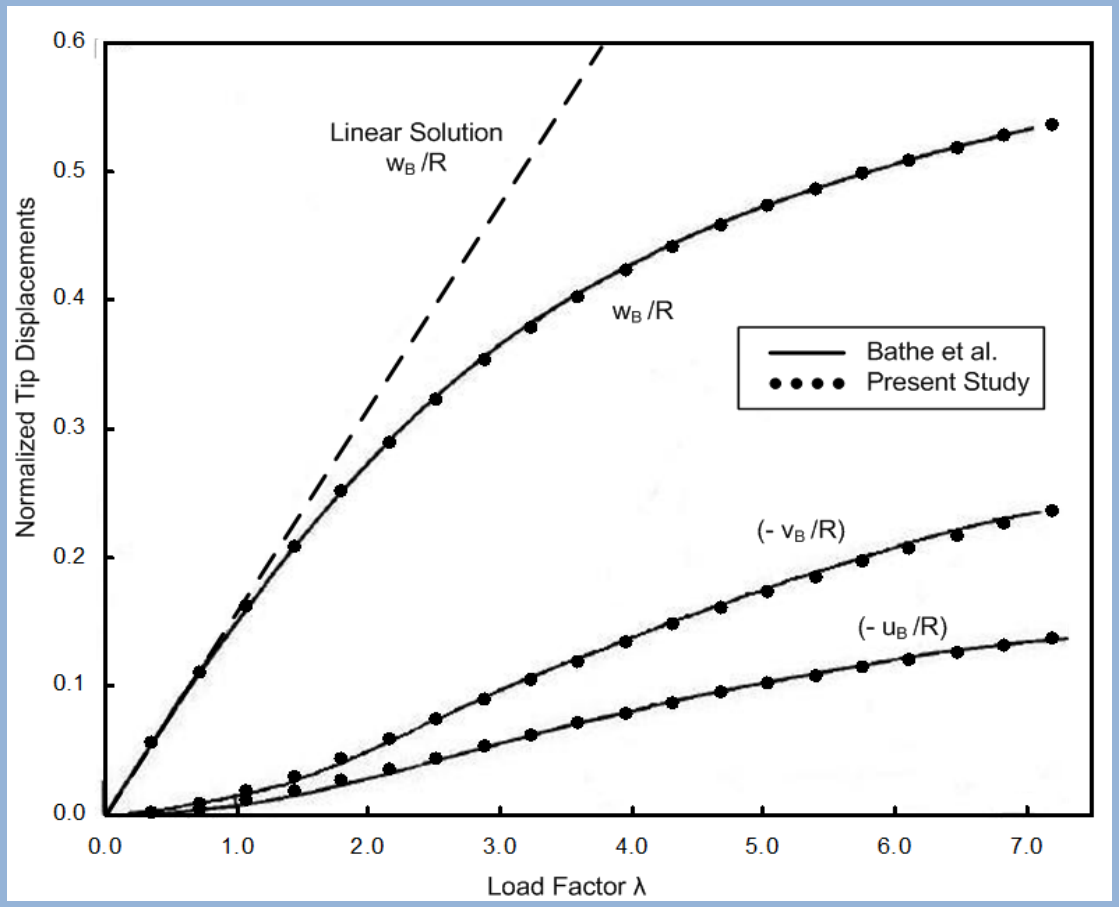

Beam Tip Displacements for Increasing Transverse Loading

Testing Examples

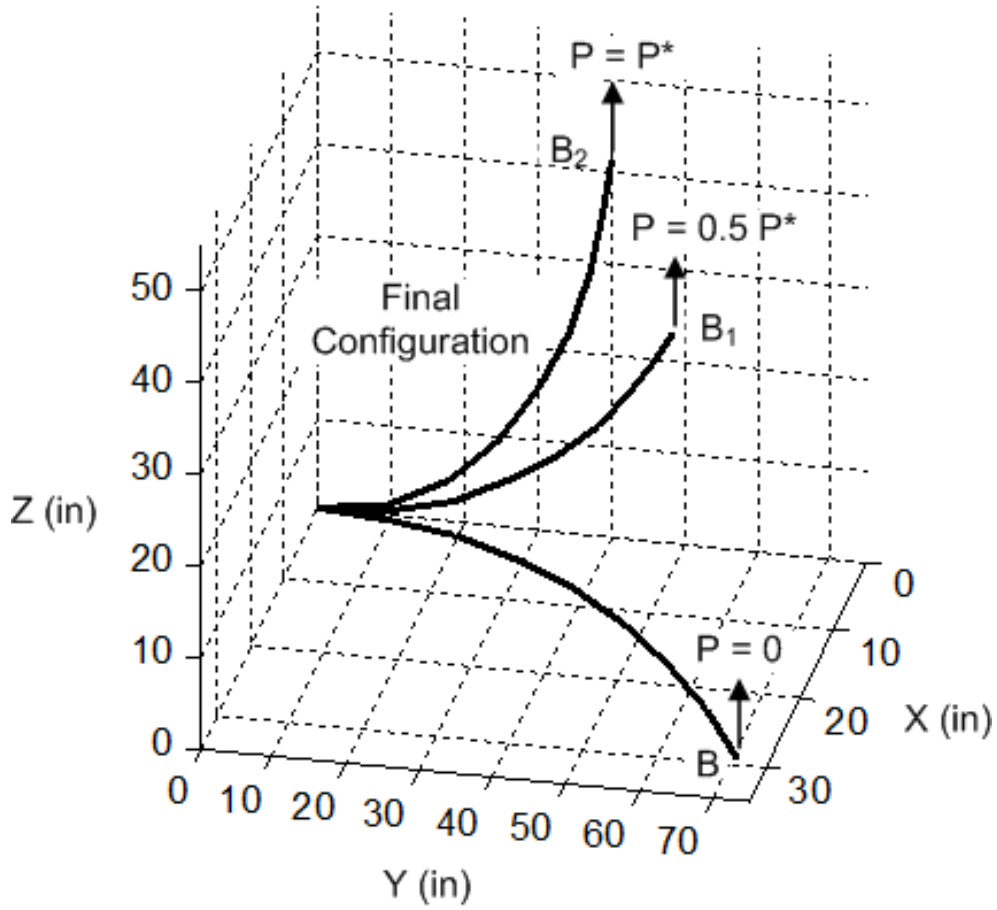

P = 0	→	B (29.3, 70.7, 0.0)
P = 0.5P*	→	B_1 (22.2, 58.8, 40.2) Present Study
	→	B_1 (22.5, 59.2, 39.5) Bathe at al.
P = P*	→	B_2 (15.6, 47.1, 53.6) Present Study
	→	B_2 (15.9, 47.2, 53.4) Bathe at al.

Beam Spatial Configurations in Large Displacement Analysis

Testing Examples

B - Dynamic Analysis

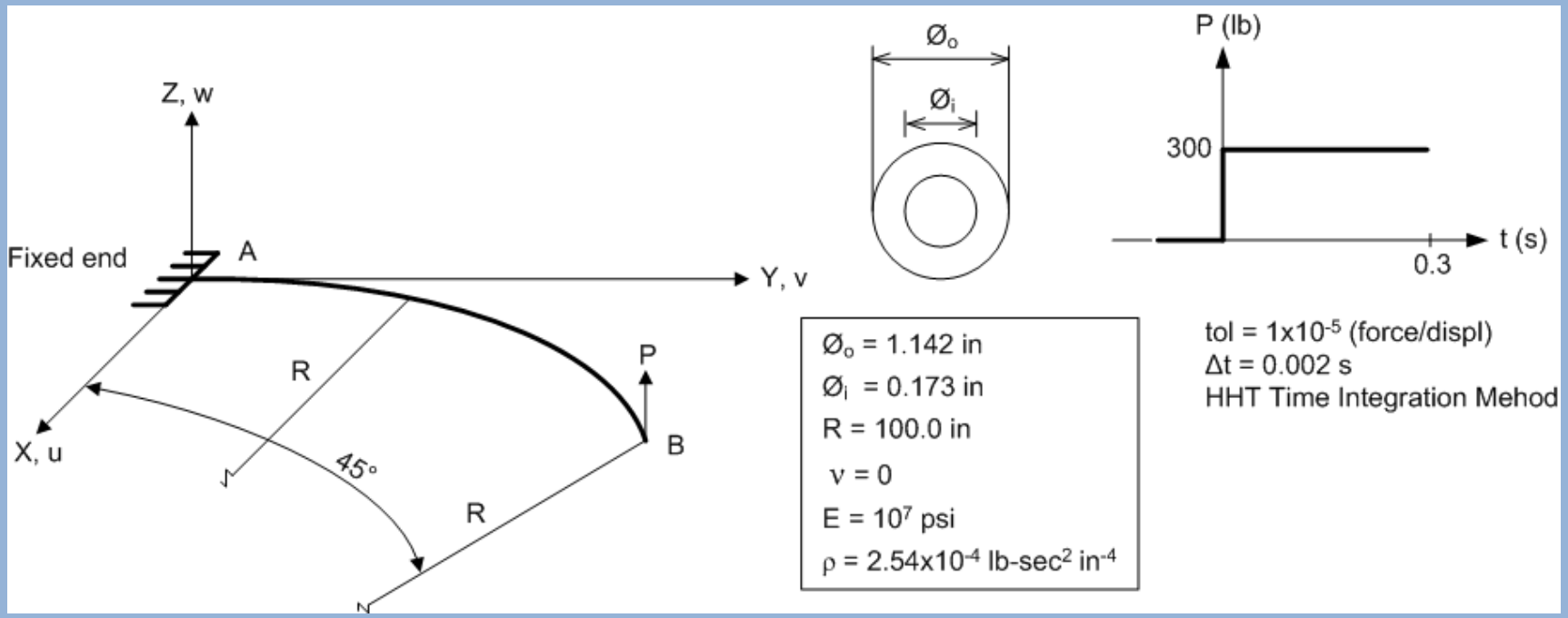

Curved Beam Under Step Loading:

Geometric, Material (Homogeneous) and Loading Characteristics

Testing Examples

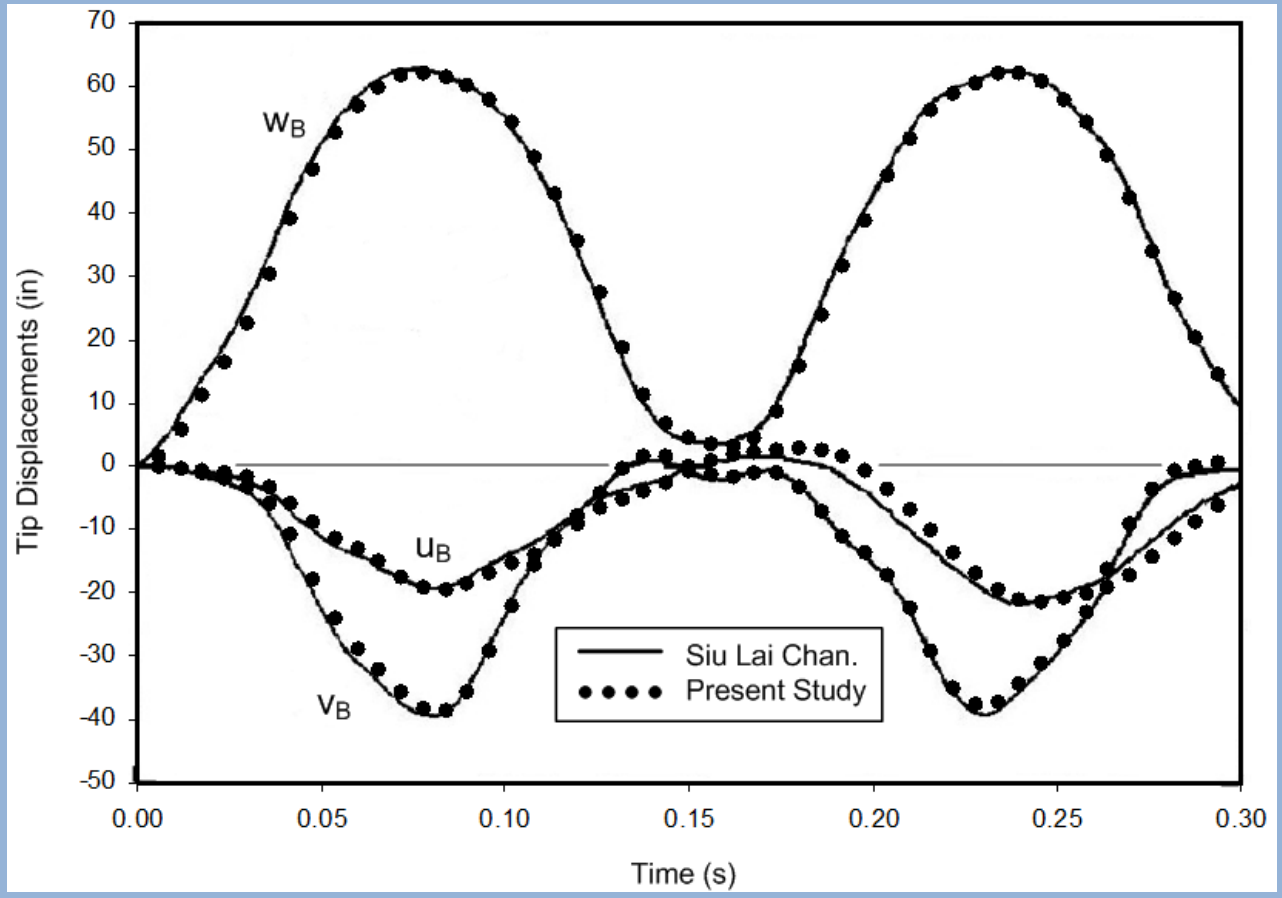

Numerical Response Comparisons of Time Varying Tip Displacements

Testing Examples

- **Dynamics of Very Long Riser**

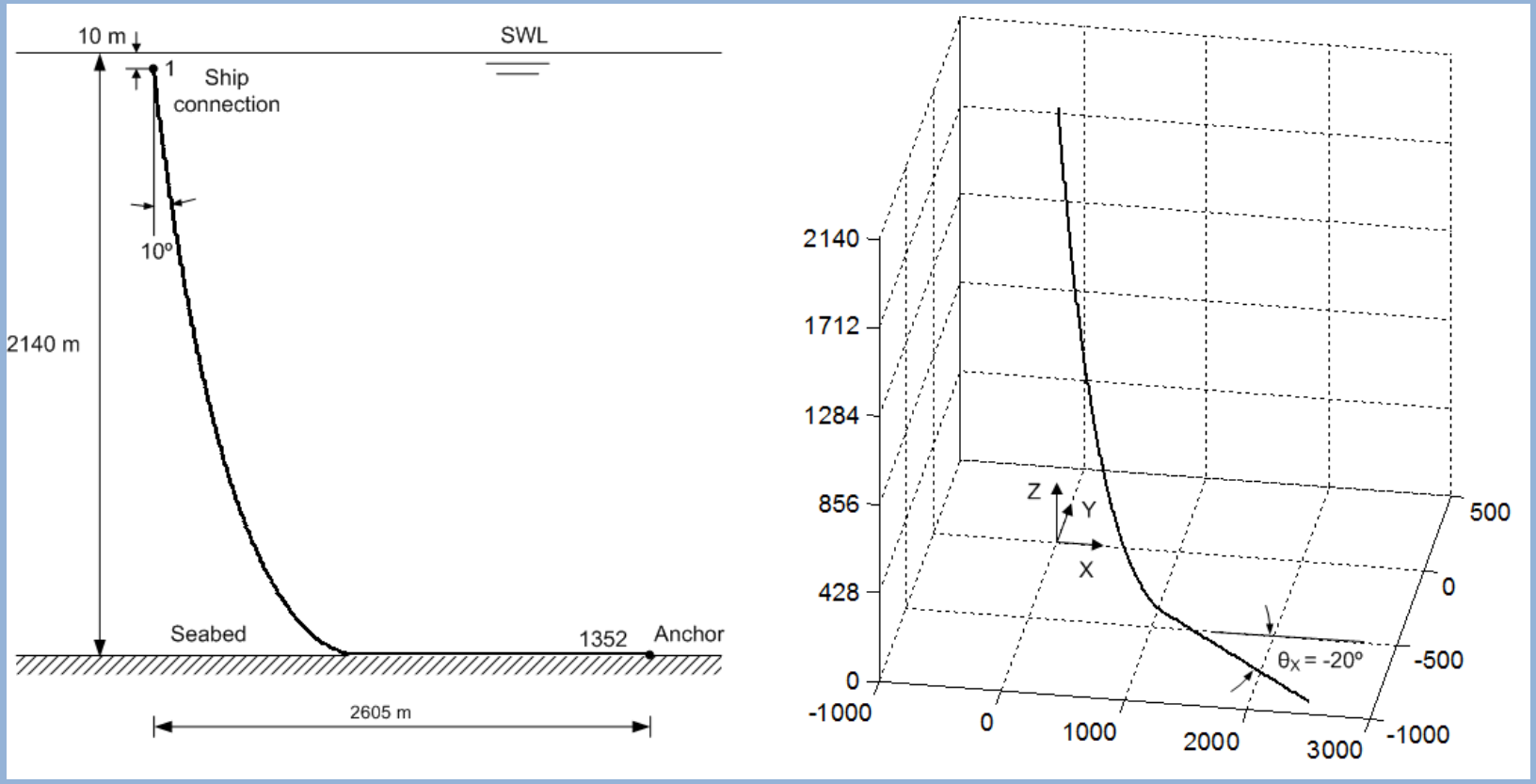

Testing Examples

Geometric, material properties and hydrostatic and hydrodynamic coefficients

Total length of the riser, L	4053 m
External diameter, Do	0.219 m
Internal diameter, Di	0.175 m
Morison's inertia coefficient, C_m	2.0
Morison's drag coefficient, C_D	1.0
Floater's weight	0.453 kN/m
Floater's bouyancy force	0.628 kN/m
Specific weight of internal fluid	6 kN/m^3
Specific weight of sea water	10.055 kN/m^3
Homogeneous Material	
Modulus of Elasticity	E = 207 GPa
Specific Weight	γ = 77 kN/m^3
FGM Material	
Modulus of Elasticity	$E = 420.7(r/r_o)^{3.126}$ GPa
Specific Weight	$\gamma = 49.2(r/r_o)^{-1.85}$ kN/m^3

Current Profile

Depth (m)	Velocity (m/s)	θ_X (deg)
0.00	1.570	180.0
1.00	1.570	180.0
4.50	1.530	180.0
40.00	1.390	180.0
340.00	0.410	180.0
740.00	0.290	270.0
1140.00	0.290	225.0
1540.00	0.290	225.0
1940.00	0.380	225.0
2140.00	0.000	225.0

Loading Properties

Static

DOF	Offset (m)
Dx	-138.397
Dy	57.326

Dynamic

DOF	Amplitude (m, deg)	Phase (deg)	Period (s)
Dx	1.025	56.886	13.242
Dy	3.054	93.042	13.242
Dz	10.794	329.870	13.242
θx	7.678	302.750	13.242
θy	1.251	230.010	13.242
θz	1.191	176.240	13.242

Testing Examples

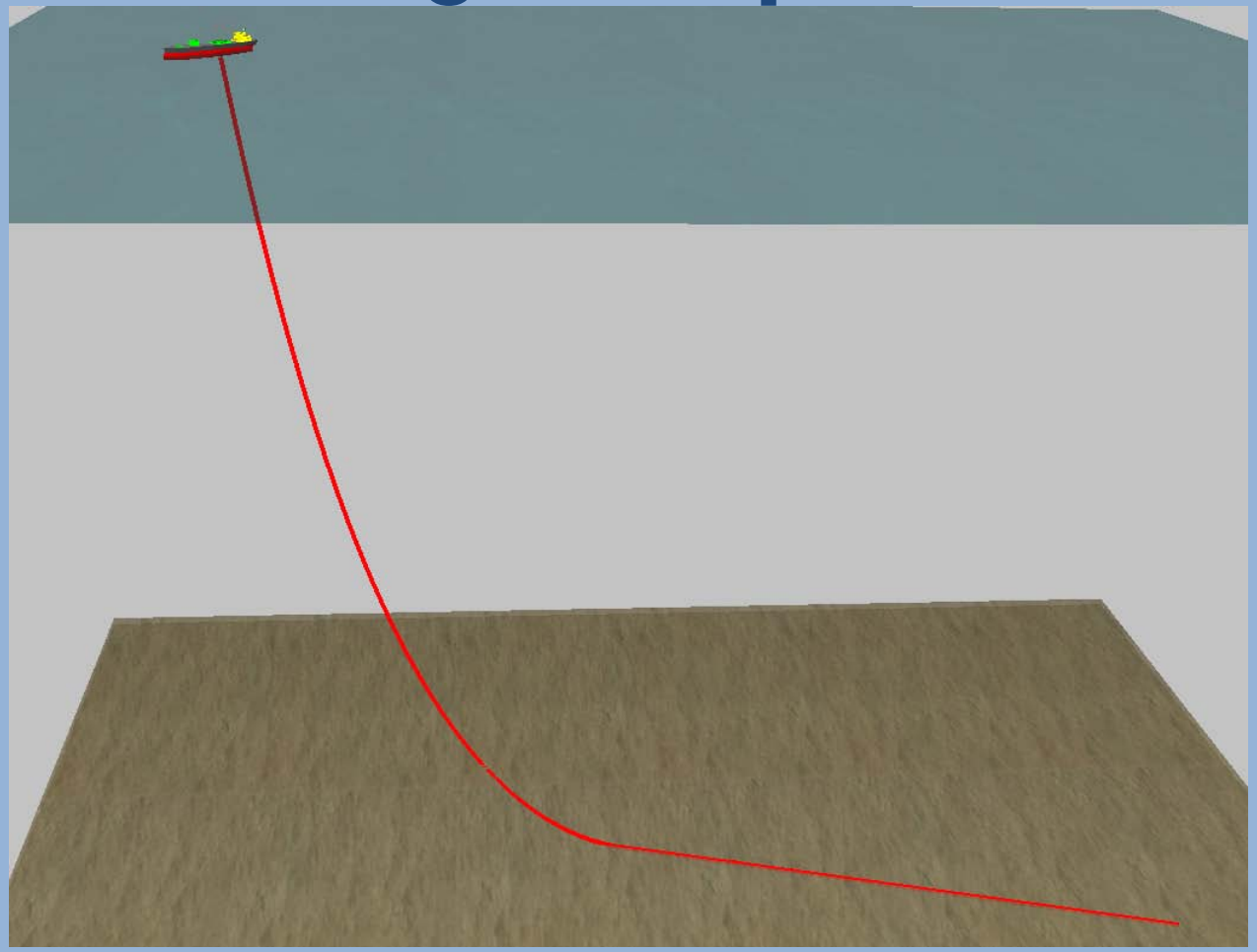

Testing Examples

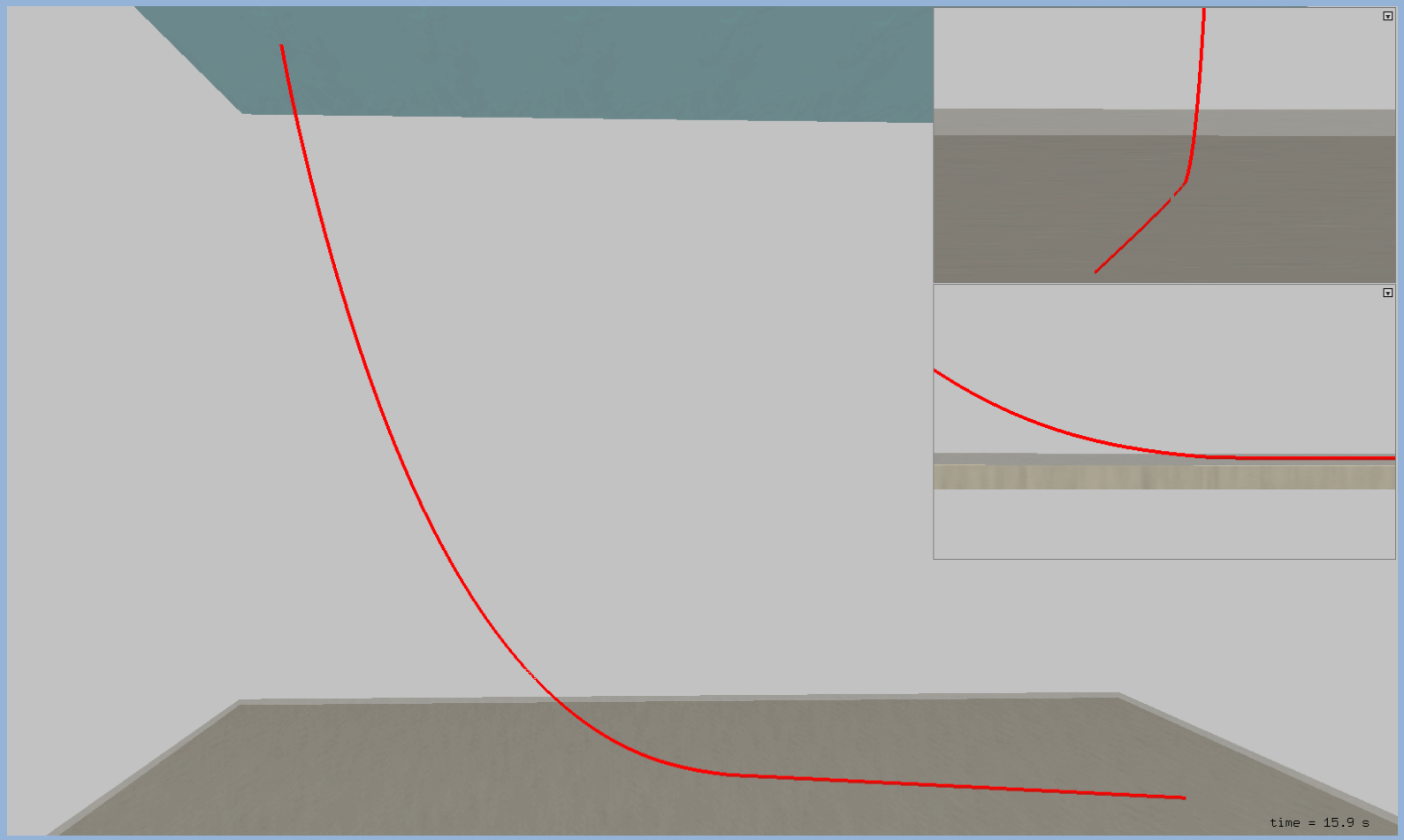

Testing Examples

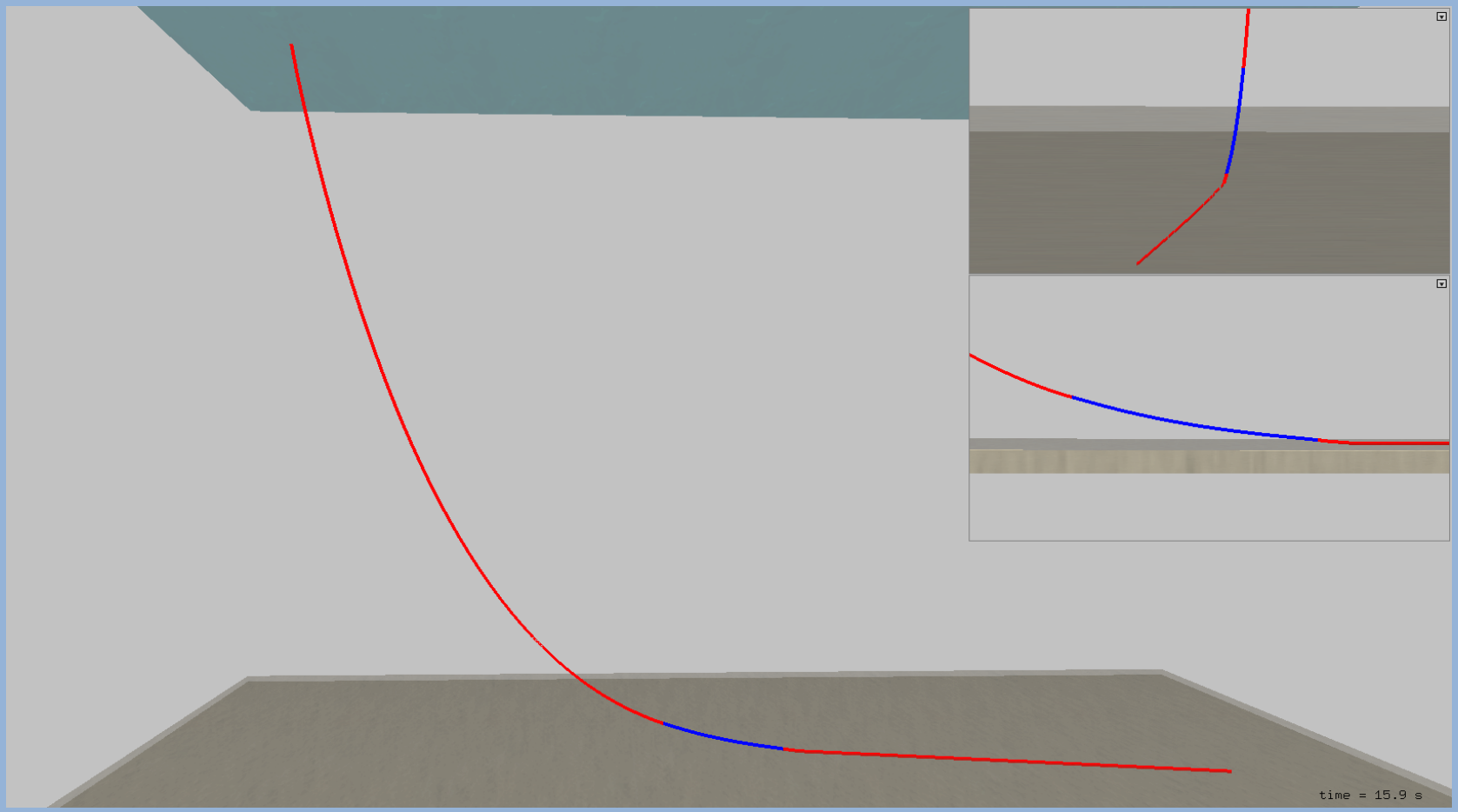

Testing Examples

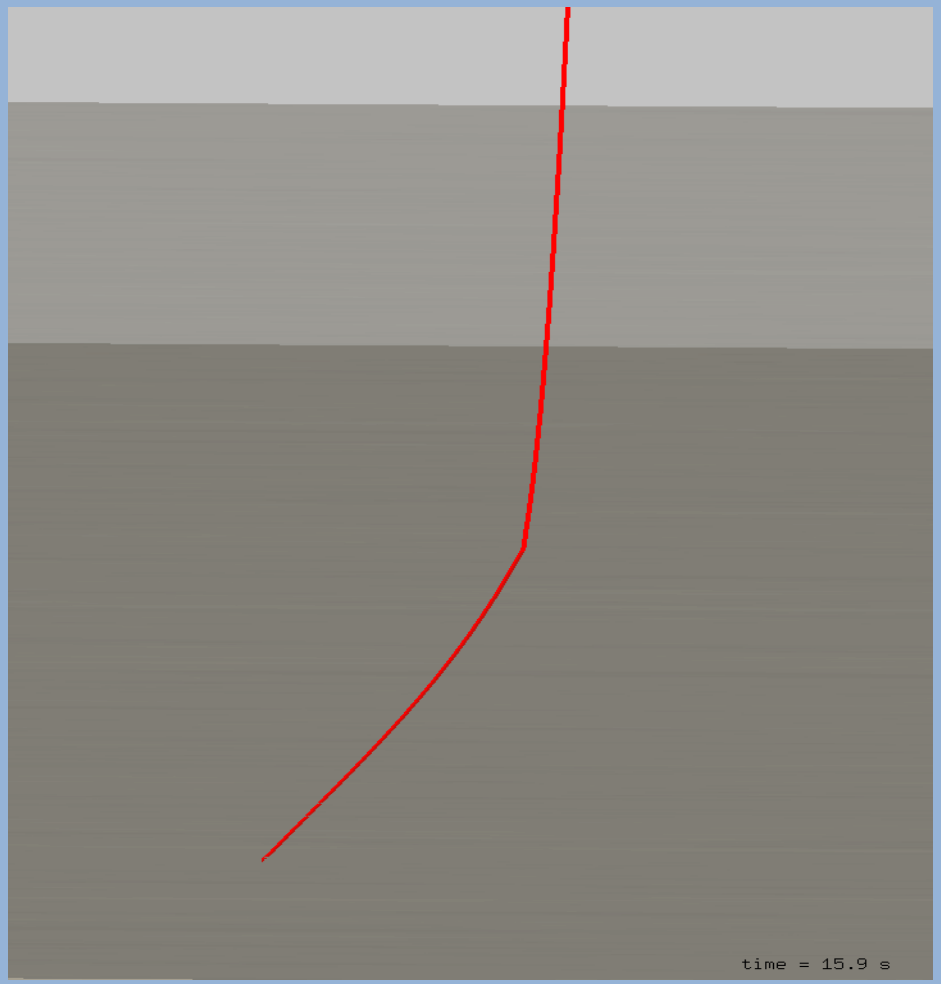

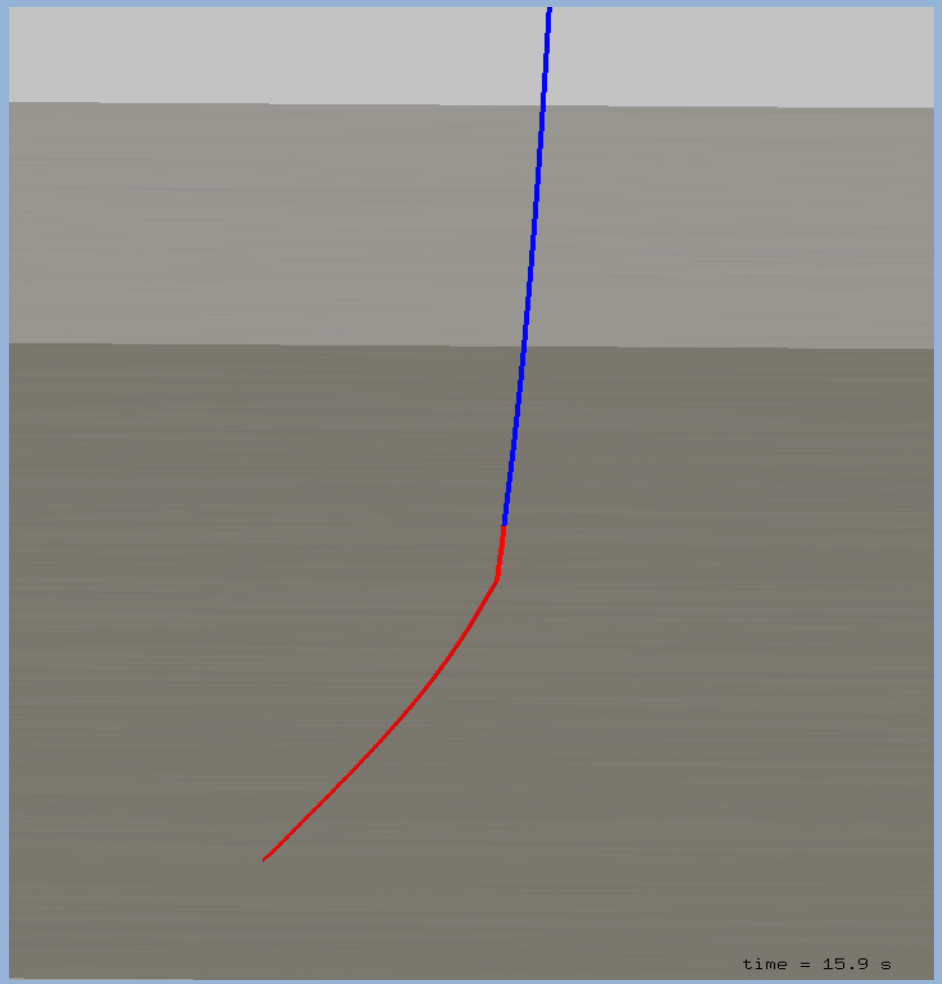

Testing Examples

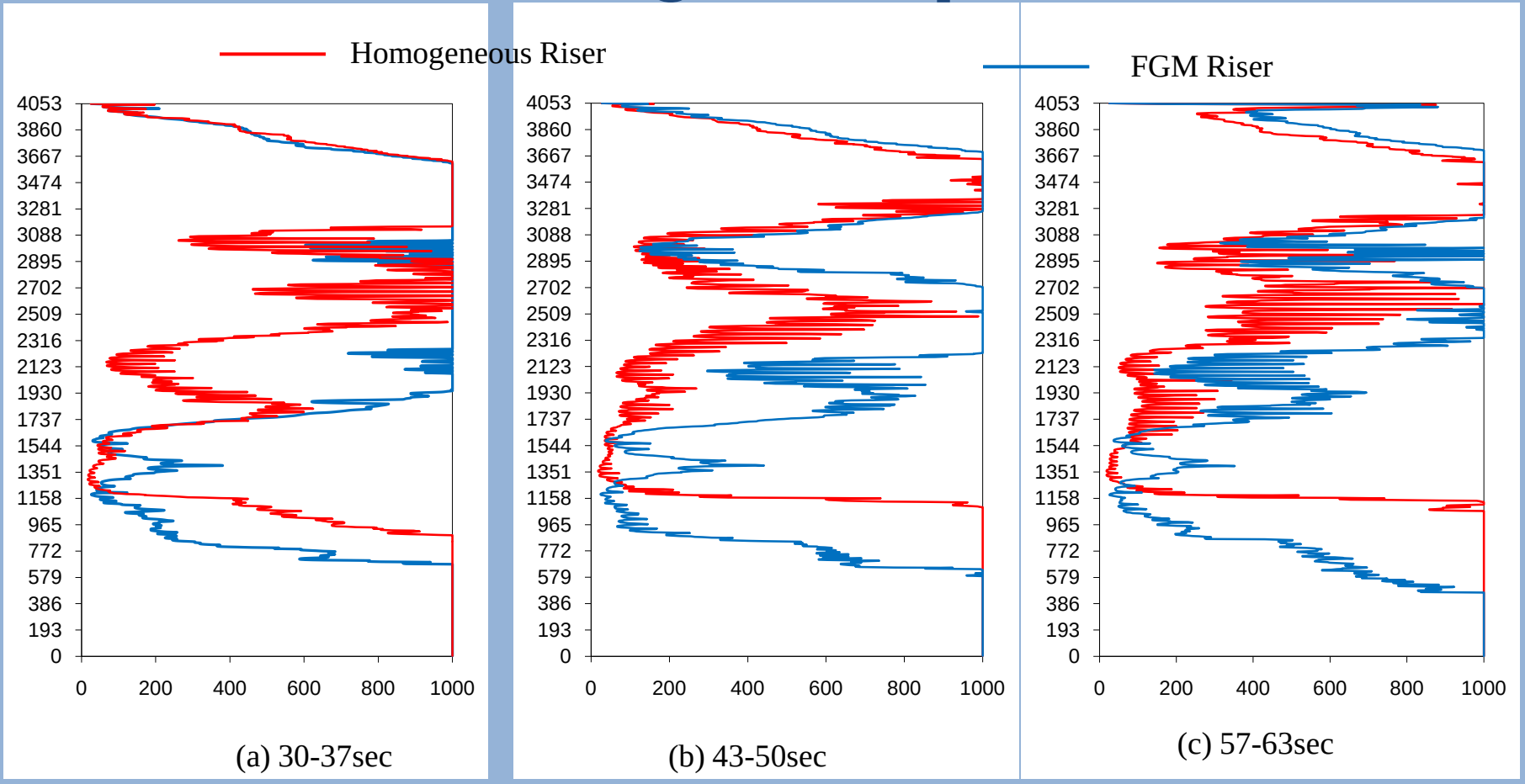

Curvature Radius Envelope at Instability Time Intervals

Testing Examples

Time Intervals	30-37sec	43-50sec	57-63sec
Homogeneous Riser	17.12 m	18.04m	18.28m
FGM Riser	26.44 m (+54%)	24.33 m (+35%)	25.91 m (+64%)

Minimum Curvature Radius Obtained From Riser Analyses

CONCLUSIONS

- General two-node beam element, based on the co-rotational formulation for geometric non-linear analysis, has been implemented and evaluated.
- FGM composed cross-sections are accounted in the model by adjusting beam rigidity parameters and considering all the cross-section evaluations in closed form.
- Significant differences in stress distributions are obtained as compared to homogeneous section beams, allowing for an effective use of FGM's in the riser design.
- Formulation applications to dynamic analyses have shown good result agreements when compared to analytical parental theoretical results, both for natural frequency evaluations as well as time incremental solutions. The use of FGM material at critical regions along the length has proven to be effective in the reduction of dynamic effects, in the riser structure responses.

Thank you
for your attention.